AGU PUBLICATIONS

JGR

Journal of Geophysical Research: Space Physics

RESEARCH ARTICLE

10.1002/2016JA023198

**Key Points:**
- Dayside reconnection can introduce a $B_y$ component into the magnetosphere, in the same sense as the IMF $B_y$
- The Dungey cycle transfers field lines with this induced $B_y$ component into the magnetotail
- The timescale for this process is found to be between 1-5 h, depending on a few contributing factors

**Correspondence to:**
S. D. Browett,
s.browett@soton.ac.uk

**Citation:**
Browett, S. D., R. C. Fear, A. Grocott, and S. E. Milan (2016), Timescales for the penetration of IMF $B_y$ into the Earth's magnetotail, *J. Geophys. Res. Space Physics*, *121*, doi:10.1002/2016JA023198.

Received 18 JUL 2016
Accepted 17 NOV 2016
Accepted article online 22 NOV 2016



# Timescales for the penetration of IMF $B_y$ into the Earth's magnetotail

**S. D. Browett[1], R. C. Fear[1], A. Grocott[2], and S. E. Milan[3,4]**

[1]Department of Physics and Astronomy, University of Southampton, Southampton, UK, [2]Department of Physics, Lancaster University, Lancaster, UK, [3]Department of Physics and Astronomy, University of Leicester, Leicester, UK, [4]Birkeland Centre for Space Sciences, University of Bergen, Bergen, Norway

**Abstract** Previous studies have shown that there is a correlation between the $B_y$ component of the interplanetary magnetic field (IMF) and the $B_y$ component observed in the magnetotail lobe and in the plasma sheet. However, studies of the effect of IMF $B_y$ on several magnetospheric processes have indicated that the $B_y$ component in the tail should depend more strongly on the recent history of the IMF $B_y$ rather than on the simultaneous measurements of the IMF. Estimates of this timescale vary from ~25 min to ~4 h. We present a statistical study of how promptly the IMF $B_y$ component is transferred into the neutral sheet, based on Cluster observations of the neutral sheet from 2001 to 2008, and solar wind data from the OMNI database. Five thousand nine hundred eighty-two neutral sheet crossings during this interval were identified, and starting with the correlation between instantaneous measurements of the IMF and the magnetotail (recently reported by Cao et al. (2014)), we vary the time delay applied to the solar wind data. Our results suggest a bimodal distribution with peaks at ~1.5 and ~3 h. The relative strength of each peak appears to be well controlled by the sign of the IMF $B_z$ component with peaks being observed at 1 h of lag time for southward IMF and up to 5 h for northward IMF conditions, and the magnitude of the solar wind velocity with peaks at 2 h of lag time for fast solar wind and 4 h for slow solar wind conditions.

## 1. Introduction

The main interaction between the solar wind and the magnetosphere is through the process of magnetic reconnection. Reconnection occurs most favorably when two oppositely directed fields in two plasmas encounter each other; this is the case at Earth when the north-south component of the interplanetary magnetic field (IMF $B_z$) is negative. Reconnection between the IMF and terrestrial magnetic field drives the dynamics of the magnetosphere through a mechanism called the Dungey cycle [*Dungey*, 1961], leading to the open magnetosphere model.

*Fairfield* [1979] showed that there is a positive correlation between the $B_y$ component in the magnetotail and the IMF $B_y$ component. $B_y$ data taken from the IMP 6 satellite of the entire breadth of the magnetotail, at 20 $R_E$ – 33 $R_E$ down the magnetotail, from 1971 to 1974 were plotted against hourly averages of measurements of IMF $B_y$. Fairfield calculated the gradient of the best fit line (the penetration efficiency) and found a weak penetration of 0.13; they did not report a value for the correlation coefficient, but the significant scatter in their Figure 9 indicates that the correlation must be low. *Cowley* [1981a] explained this observation as a consequence of the open magnetosphere model. Newly opened field lines on the dayside have a $B_y$ component, which is transferred into the magnetotail lobes as the field lines convect into the lobes. The $B_y$ asymmetry is then transferred onto closed field lines when the asymmetric lobe field lines undergo magnetotail reconnection. The word "penetration," in terms of the IMF exerting an influence on magnetospheric field lines, can be misleading. The IMF does not enter the magnetosphere; instead, the field lines associated with the IMF connect to magnetospheric field lines which then allow the IMF to act upon the magnetosphere, inducing a $B_y$ component in the magnetosphere in the same sense as in the IMF. The choice to use the word "penetration" is for consistency in terminology with previous studies.

Since *Fairfield* [1979] there have been further studies showing the correlation between instantaneous measurement of the IMF $B_y$ and the magnetotail $B_y$ [*Tsurutani et al.*, 1984; *Hilmer and Voigt*, 1987; *Nagai*, 1987; *Sergeev*, 1987; *Voigt and Hilmer*, 1987; *Hau and Erickson*, 1995; *Newell et al.*, 1995; *Wing et al.*, 1995; *Petrukovich*, 2009] which have reported penetration efficiencies ranging from 0.1 to 0.6; a review by *Kaymaz et al.* [1994]

is also available. *Nishida et al.* [1995] has reported a penetration efficiency of 0.25 in the distant tail during instances of lobe reconnection (northward IMF) with a dominant IMF $B_y$ component. A mechanism for IMF penetration under northward IMF conditions, which explains the observations made by *Nishida et al.* [1995], has been proposed in *Nishida et al.* [1998] and simulated in *Nishida and Ogino* [1998]. Other studies have investigated how IMF $B_y$ affects the polar cap convection cell pattern [*Moses et al.*, 1985].

*Petrukovich* [2011] discussed the sources of $B_y$ components in the magnetotail; they found that the largest source of $B_y$ in the magnetotail is from IMF $B_y$ penetration and listed the following (more minor) effects:

1. Magnetotail flaring is the effect where magnetospheric magnetic field lines are connected to the ionosphere, and therefore, away from the magnetotail axis, they have a $B_y$ component. Petrukovich estimates that at $Y_{GSM} = \pm 10 R_E$ there will be an addition of plasma sheet $B_y$ that is approximately equal to 40% of the plasma sheet $B_x$ component. This effect is equal and opposite in the northern and southern hemispheres and so it cancels out at the neutral sheet (the interface between the inward and outward pointing field lines of the northern and southern hemispheres, respectively).
2. Neutral sheet warping is the situation where the flanks of the neutral sheet warp southward and the center of the neutral sheet deflects northward in the summer, and oppositely for the winter. This effect is relatively small, having been estimated by *Petrukovich* [2011] to contribute approximately $\pm 1.75$ nT to the $B_y$ component in the plasma sheet.
3. Another addition of $B_y$ into the magnetotail is due to the even tilt effect, where the neutral sheet twists to remain normal to the line connecting each end of the dipole. This means that the even tilt effect is positively correlated with the orientation of the dipole tilt. It has been estimated [*Petrukovich*, 2011] that this effect contributes up to 2 nT to the $B_y$ component of the plasma sheet.
4. Magnetotail twisting occurs when IMF field lines with a $B_y$ component open the Earth's magnetic field lines (through reconnection) and exert a torque which acts to straighten the open field lines by twisting the magnetotail. *Petrukovich* [2011] estimates that this effect induces an additional $B_y$ component to the plasma sheet that is approximately equal to 10% of the IMF $B_y$ component. *Petrukovich* [2011] states however that this source of $B_y$ in the magnetotail can be considered as a part of IMF penetration as it also is solely dependent on IMF $B_y$.

To measure these effects, Petrukovich performed his analysis in geocentric solar wind (GSW) coordinates in which the $x$ axis is antiparallel to the solar wind flow direction and the $x$-$z$ plane is defined to contain the dipole axis so that only external effects on the magnetotail are measured. Petrukovich also found that the difference between GSW and GSM coordinates (whose $x$-$z$ plane also contains the dipole axis but the $x$ axis is directed toward the Sun) is marginal, and so performing the analysis in GSM coordinates does not offer any disadvantage in the accuracy of the analysis.

The correlation of magnetotail $B_y$ with IMF $B_y$ was further examined by *Cao et al.* [2014]. Cao et al. specifically restricted their study to the $B_y$ component observed at the neutral sheet and used several criteria to look exclusively at the neutral sheet during geomagnetically quiet conditions. By studying the $B_y$ component at the neutral sheet Cao et al. excluded $B_y$ contribution from magnetotail flaring as the flaring components on either side of the neutral sheet are equal and opposite. By using data taken at the neutral sheet and ignoring the relatively small $B_y$ components induced by neutral sheet warping, magnetotail twisting, and the even tilt effect, the contribution from only magnetotail penetration is measured. Cao et al. defined "quiet conditions" as when there were (i) no changes in solar wind dynamic pressure (either in relative or absolute terms) within 5 min of a neutral sheet crossing, (ii) no changes in the sign of the IMF $B_z$ component within 5 min of a neutral sheet crossing, and (iii) no fast flows in the neutral sheet at the time of a neutral sheet crossing. Cao et al. found that by restricting their study to the neutral sheet, and by implementing these criteria, a much higher penetration efficiency was found: 0.72 compared to 0.13 in *Fairfield* [1979].

Most of the above studies have investigated the link between $B_y$ values observed in the magnetotail and the instantaneous IMF $B_y$ component (averaging up to a 1 h lag time). However, it has been estimated that the Dungey cycle of reconnection should take on the order of a few hours for a field line to convect from the dayside into the magnetotail [*Dungey*, 1965; *Cowley*, 1981b; *Fear and Milan*, 2012a], though this estimate has been rarely tested directly. One way in which the timescales associated with the Dungey cycle have been indirectly investigated is through the study of transpolar arcs. Transpolar arcs are Sun-aligned large-scale auroral features which form in the polar cap during periods of northward IMF [*Frank et al.*, 1982]. It has been argued that they are formed by the process of magnetotail reconnection during periods of northward IMF and hence

that the local time at which a transpolar arc forms should depend on the $B_y$ component at the neutral sheet which in turn should depend on the recent history of the IMF $B_y$ component [*Milan et al.*, 2005]. *Fear and Milan* [2012a, 2012b] carried out a statistical study into the formation of 131 transpolar arcs and showed that the magnetic local times at which transpolar arcs formed was more strongly dependent on the IMF 3–4 h before the arc formed, which was argued to be indicative of the timescales taken for field lines to convect from the dayside magnetopause to the neutral sheet. However, although the observed correlation between the magnetic local time at which the transpolar arcs formed and the IMF $B_y$ component peaked when the IMF was lagged by 3–4 h, the correlation was elevated compared with its zero-lag value over a wide range of lag times, from 1 to 10 h. *Grocott and Milan* [2014] have incorporated timescales into a study on the morphology of ionospheric convection patterns. They produced average convection patterns for different IMF clock angles, where those clock angles were also binned according to how long the IMF had remained in that orientation. They observed that the convection cell patterns begin to respond within 30 min of constant IMF conditions with the convection cell patterns continuing to evolve on the order of hours of constant IMF clock angle. A timescale of hours is in agreement with arguments put forward by *Dungey* [1965], *Cowley* [1981b], and *Fear and Milan* [2012a] who argue that the convection of magnetic field lines from the dayside to the nightside should take a small number of hours; if the *Cowley* [1981a] interpretation is correct, then evidence for such timescales should be present when the magnetotail $B_y$ component is correlated with the recent history of the IMF $B_y$ component. Other aspects of magnetospheric timescales have also been investigated. *Cao et al.* [2013] investigated the timescales associated with energetic proton fluxes in the central plasma sheet. They found a correlation with the magnitude of IMF $B_z$ when the IMF was southward, which was stronger if the IMF was lagged by 40–100 min. (No correlation was found when the IMF was northward.) However, this is not a measure of the Dungey cycle timescale; the authors interpret the delay as indicative of the timescale for energy accumulation by addition of magnetic flux into the lobe (which does not correspond to the full convection of a field line from the dayside to nightside reconnection sites).

Two recent studies have made more direct measurements of the timescales associated with IMF penetration. *Rong et al.* [2015] carried out two case studies of events where strong (5 nT) variations in the IMF $B_y$ component were identified with subsequent magnetotail plasma sheet $B_y$ fluctuation in the same sense as the IMF. A lag time of 1–1.5 h was found. An alternative approach was taken by *Zhang et al.* [2015], who carried out a study of polar cap patches during a small geomagnetic storm. The patches were tracked as they convected across the polar cap and returned at lower latitudes as part of the Dungey cycle. The timescales taken for the polar cap patches to convect from noon to midnight in MLT were approximately 1–2 h, in agreement with *Rong et al.* [2015] but slightly shorter than those found by *Fear and Milan* [2012a]. One possible explanation for the apparent disagreement with the convection timescales from these three studies is the differences in the IMF conditions. In the *Zhang et al.* [2015] and *Rong et al.* [2015] case studies, the IMF $B_z$ was negative or around zero respectively, whereas *Fear and Milan* [2012a] were considering periods when transpolar arcs were present, and hence the IMF was northward. The different IMF conditions in these studies indicate different levels of dayside reconnection and hence different levels of driving of magnetospheric convection. One would expect timescales for magnetospheric convection under northward IMF conditions to be longer than when the IMF is southward.

If the *Cowley* [1981a] interpretation is correct, the above results suggest that a closer correlation between the IMF $B_y$ and plasma sheet $B_y$ should be achieved with the inclusion of a lag. Conversely, it has been suggested that field lines which reconnect to the solar wind do not need to convect across the polar cap and undergo nightside reconnection to introduce a $B_y$ component into the neutral sheet. *Tenfjord et al.* [2015] has recently suggested that when magnetospheric field lines undergo dayside reconnection, a perturbation is introduced into the magnetosphere which forms a compressional MHD wave which propagates through the magnetosphere much more quickly than field lines can convect. They argue that the introduced perturbation has an asymmetry between the northern and southern hemispheres that is in the same sense as the IMF; this means that a $B_y$ component can be introduced into the magnetotail by this process on a timescale of approximately 25 min.

In this study we extend the analysis of *Cao et al.* [2014] to include time dependencies; in doing so we investigate statistically the timescales required for the IMF $B_y$ component to penetrate fully into the magnetosphere. In this way, we expect to be able to identify the relative contributions of the mechanisms for penetration outlined by *Cowley* [1981a] and *Tenfjord et al.* [2015]. If the timescales are determined to be

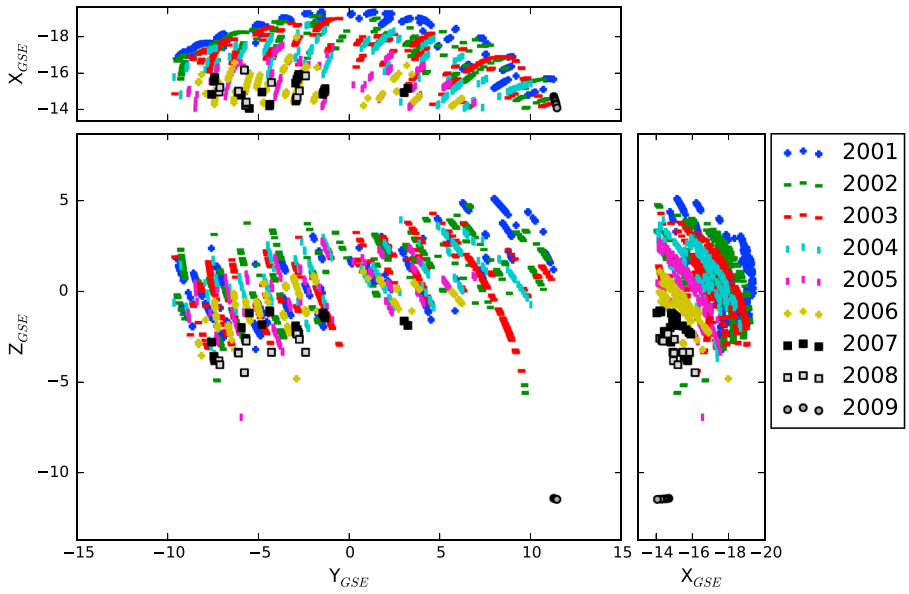


**Figure 1.** Locations of all 5030 neutral sheet crossings from 2001 to 2009, identified by sign reversals of the $B_x$ component in the plasma sheet.

mainly convection-driven processes, rather than pressure effects, then our observations will act as a means of identifying the timescales intrinsic to magnetospheric convection.

## 2. Instrumentation

In order to adopt the same approach as *Cao et al.* [2014], neutral sheet crossings were identified in the data from Cluster 3 between 2001 and 2009. In order to identify the crossings, we examined spin (4 s) resolution data from the fluxgate magnetometer instrument (FGM) [*Balogh et al.*, 2001; *Gloag et al.*, 2010]. Data from the Cluster Ion Spectrometer Hot Ion Analyzer (CIS-HIA) [*Rème et al.*, 2001; *Dandouras et al.*, 2010] were used to identify the presence or absence of fast flows in the plasma sheet. The OMNI database was used to provide 1 min resolution data on the solar wind conditions, specifically the IMF vectors and solar wind dynamical pressure [*King and Papitashvili*, 2005].

## 3. Event Identification

In order to identify neutral sheet crossings, we identified reversals in the $B_x$ component observed by Cluster 3 in the same spatial region as used by *Cao et al.* [2014]: $-14\,R_E > x_{GSM} > -19.6R_E$ (where $-19.6R_E$ is the apogee of the spacecraft) and $-9\,R_E < y_{GSM} < 11\,R_E$. The geocentric solar magnetospheric (GSM) coordinate system was used for this analysis as the *x*-*z* plane contains the dipole axis of the magnetosphere which removes internal mechanisms for addition of $B_y$ in the plasma sheet. Excluding magnetotail $B_x$ sign reversals which straddle data gaps of greater than 5 s, we identified 6030 crossings, the locations of which are shown in Figure 1. As the neutral sheet is the boundary between the northern and southern hemispheres of the magnetotail, we expect the locations of the neutral sheet crossings to be around zero on the *z* axis. Although there was not an explicit *z* range criterion applied, most of the crossings fall in the range of $\pm 8R_E$ around zero on the *z* axis. The exception is the small collection of points at [−14, 11, −15] $R_E$, which are all the potential event detections identified from 2009. All of the identified events in 2009 occurred on the same orbit (11 October 2009 at 03:30–05:30UT). Examination of the in situ data from this orbit reveals that the spacecraft was situated in the magnetosheath, as indicated by the lower energies of the ion population (Figure 2a, panel i) and the consistently fast ion velocity (Figure 2a, panel v) in the 2009 events compared to the corresponding panels in the sample data taken from 2001 (Figure 2b). Therefore, all events identified in 2009 were excluded, which leaves 5982 neutral sheet crossings for analysis. For each of the remaining neutral sheet crossings the magnetotail $B_y$ component at the neutral sheet was determined by taking the mean of the $B_y$ measurement immediately before and immediately after the $B_x$ sign reversal. By taking only $B_y$ data from the neutral sheet, the addition of magnetotail $B_y$ from magnetotail flaring effects, as discussed in section 1, has been removed. Through a

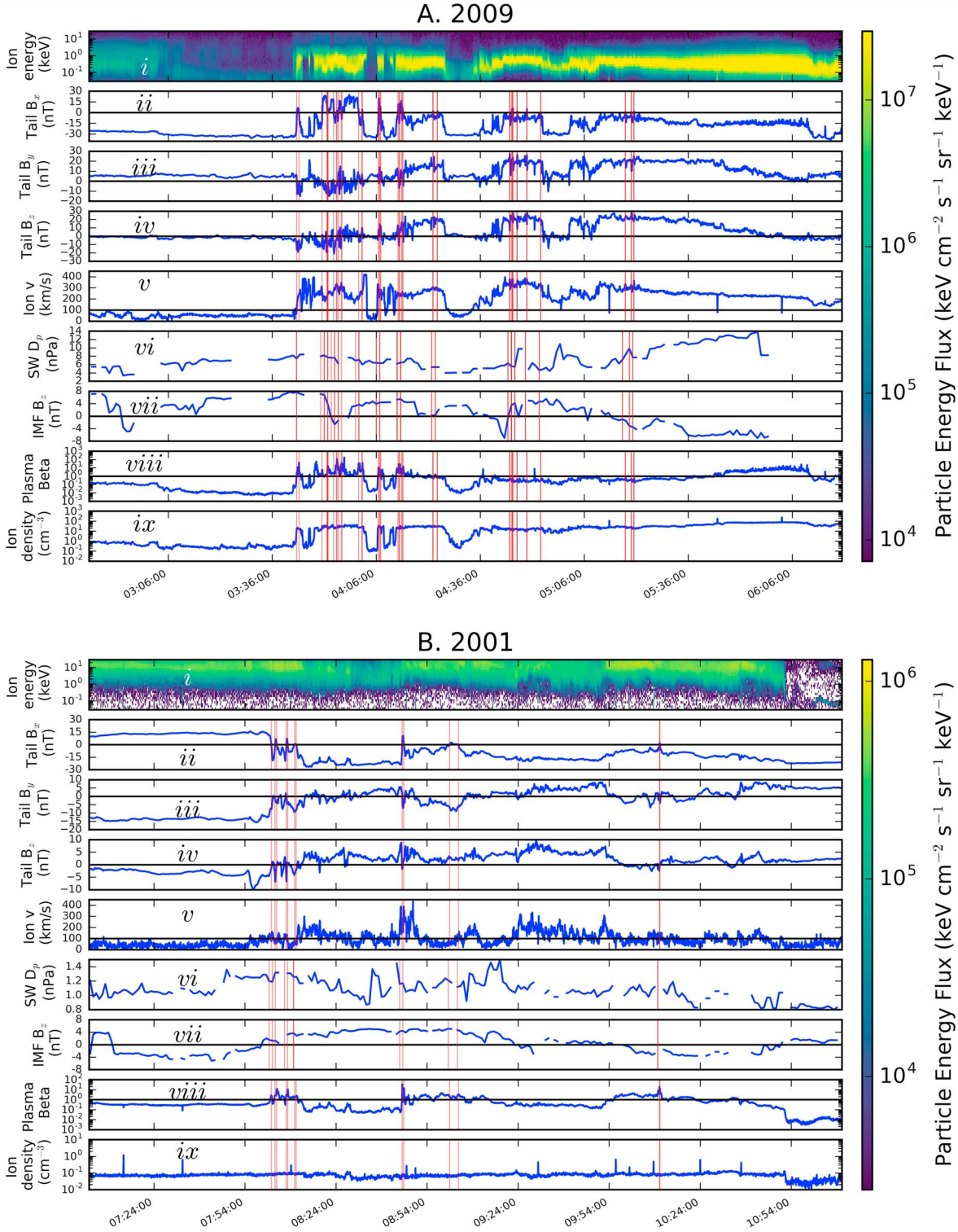


**Figure 2.** (a) Key parameters of all (48) candidate neutral sheet crossings observed by Cluster 3 on 11 October 2009. (b) All the events from an exemplar orbit from 2001, which were observed on 13 October 2001. For each year, (i) a spectrogram of the ion energies; the (ii) $B_x$, (iii) $B_y$, and (iv) $B_z$ components of the magnetic field in the plasma sheet; (v) the ion velocities; (vi) the solar wind dynamical pressure; (vii) the IMF $B_z$ component; (viii) the plasma beta; and (ix) the plasma density. Note that the *y* axis scales for most panels differ between years. Data shown are from Cluster 3, except for the solar wind dynamic pressure and IMF $B_z$ component which are taken from the OMNI database. The time of each event shown is indicated by a vertical red line. The spectrograms observed in both years show that the events from 2009 have a much lower ion energy than in 2001. Coupled with the observation that the events in 2009 occurred much farther away from the equatorial plane than the other events (at [−14, 11, −15] $R_e$), this is indicative that these events are from the magnetosheath which is outside of the magnetosphere.

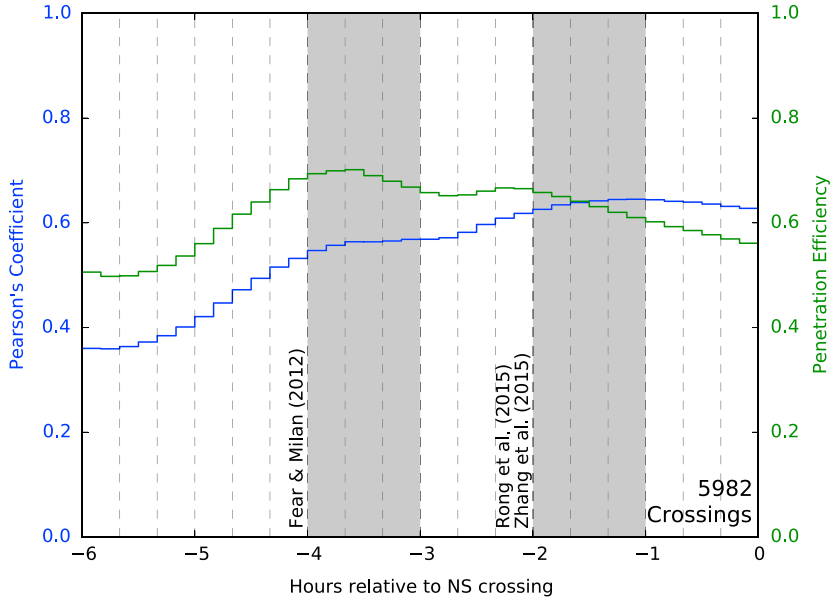


**Figure 3.** Correlation time series plot for all neutral sheet crossings. The blue series shows how the correlation coefficient varies as the IMF $B_y$ data are lagged relative to the plasma sheet $B_y$ data. The green series shows how the penetration efficiency changes as the lag applied to the IMF $B_y$ data is varied. Peaks are seen at approximately 1–2 h and 3–4 h which are consistent with previous studies, indicated by grey shading.

combination of adopting GSM coordinates and taking data from the neutral sheet, we have eliminated the largest sources of plasma sheet $B_y$ other than by IMF penetration.

## 4. Investigation of Lag Times

As an initial step, to correlate the neutral sheet crossing $B_y$ measurements with the IMF $B_y$ conditions, the IMF $B_y$ component was averaged over an hour leading up to each neutral sheet crossing (based on the 1 min resolution OMNI data). These hour averages were then correlated with the measurements in the neutral sheet using the Pearson's correlation coefficient, and the gradient from the least squares trend line is defined as the penetration efficiency [*Fairfield*, 1979]. The penetration efficiency is calculated as it is a measure of how closely the IMF and neutral sheet are related; if the IMF $B_y$ component penetrates into the magnetotail with 100% efficiency and with no other additions of $B_y$ in the neutral sheet, the gradient of the best fit trend line will become 1. The correlation coefficient is a measure of how much scatter there is in the data from the best fit trend line. When calculating these values for all of the neutral sheet crossings in our observing region, we find the correlation coefficient and penetration efficiency to be 0.63 and 0.56, respectively.

Once the $B_y$ components from the neutral sheet crossings were correlated with instantaneous measurements of the IMF $B_y$ components, the effect of IMF $B_y$ over longer timescales was investigated. This was done by averaging the IMF $B_y$ data over an hour leading up to 10 min before the corresponding neutral sheet crossing and finding the correlation coefficient and penetration efficiency of this lagged average of the IMF $B_y$ with the neutral sheet $B_y$. The 1 h window (used to calculate the hour average) was then moved progressively earlier in 10 min steps up to a maximum of 6 h (i.e., the longest delay considered related to a 1 h window which ended 6 h before the neutral sheet crossing). In this way, we build up a picture of how the correlation coefficient and penetration efficiency evolves over that 6 h time period. Figure 3 shows how the correlation coefficient and penetration efficiency of the IMF into the magnetotail vary over this 6 h time period with the shaded regions highlighting the lag times reported by previous studies (labeled). The values quoted above for the correlation coefficient and penetration efficiency, with no lag applied to the solar wind data, correspond to the values of the time series at the right-hand side of the figure. As the applied lag increases (from right to left in the figure), the correlation coefficient peaks at a solar wind lag of 1 h and then decreases and plateaus at 3 h. The penetration efficiency shows a clearer double-peak feature with local maxima at about 2 h and 3 h 40 min. The reason for this double feature is discussed in section 6. For context, we interpret the penetration efficiency as a measure of how closely the IMF controls the magnetotail, as the closer the measurements of

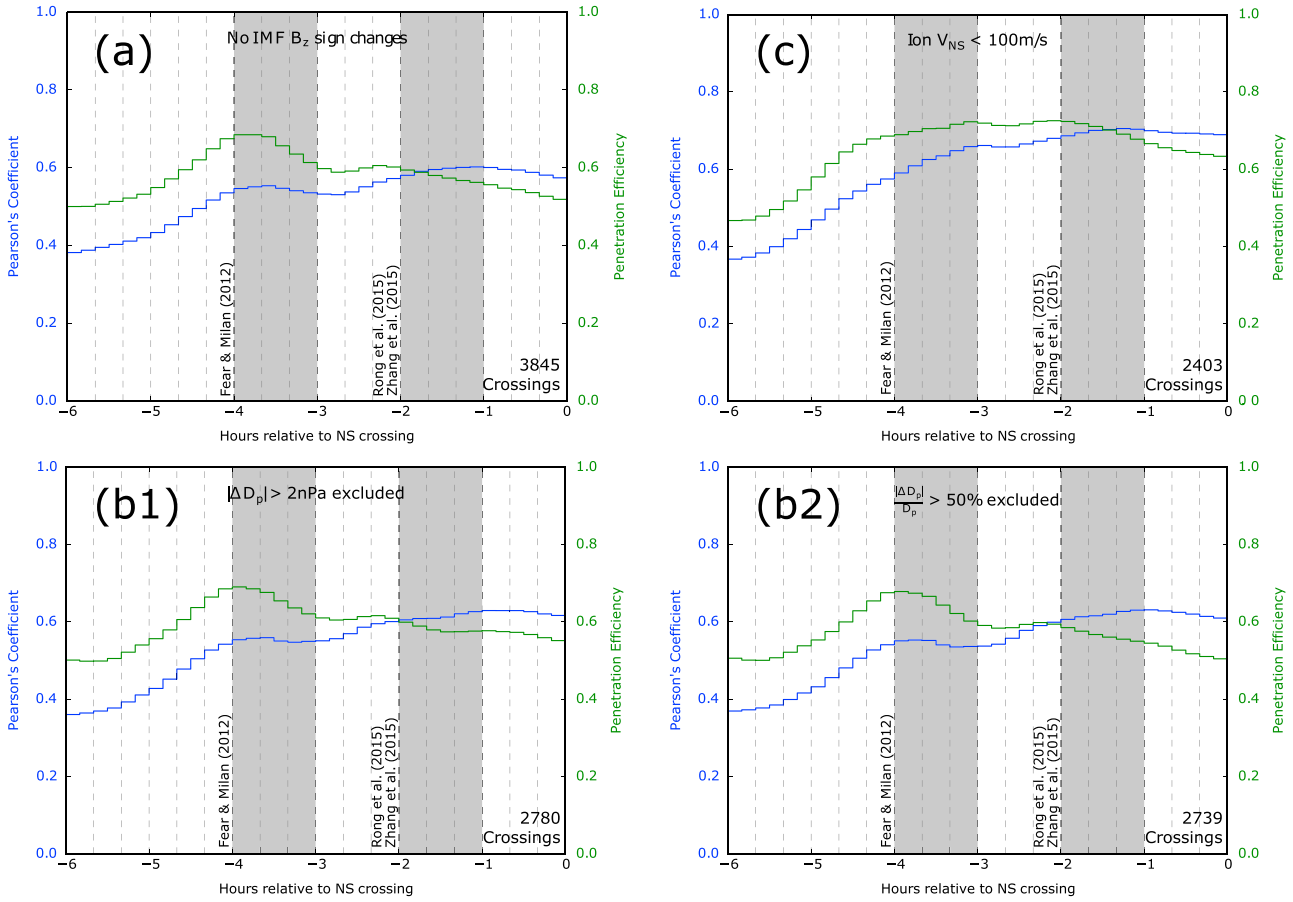


**Figure 4.** Each panel is in the same format as in Figure 3 but shows the effects of applying each of the filters chosen by *Cao et al.* [2014]. (a) All events except those with an IMF $B_z$ sign change in the 5 min before or after a neutral sheet crossing is excluded; (b1) all events except those where there was a change in the solar wind dynamical pressure of 2 nPa within 5 min of a neutral sheet crossing; (b2) all events except those where there were relative solar wind pressure changes of more than 50% in the same 10 min window; and (c) all events except for those with fast ion flows (>100 m $s^{-1}$) in the magnetotail at the time of the neutral sheet crossing have been excluded.

the IMF and magnetotail are the closer the penetration efficiency gets to 1. We also interpret the correlation coefficient as a measure of scatter on the data. In the following sections, we will show that as criteria based on the interplanetary conditions are applied, the traces of penetration efficiency and correlation coefficient match more closely, indicating a higher degree of control (i.e., less scatter) as the data are subsetted.

## 5. Event Filtering

In order to investigate the impact of magnetospheric convection on the timescales evident in Figure 3, we applied the criteria outlined by *Cao et al.* [2014] to the neutral sheet crossings in order to exclude intervals of change in the magnetosphere (IMF $B_z$ sign changes, solar wind pressure pulses, and neutral sheet crossings that were observed at the same time as fast flows in the magnetotail). Below we consider the effect of each of these in turn.

### 5.1. IMF $B_z$ Sign Changes

*Li et al.* [2011] suggested that a change in the sign of the IMF $B_z$ component can introduce a strong disturbance into the magnetosphere; therefore, *Cao et al.* [2014] chose to consider only periods of steady convection (at whatever rate). To do this, they excluded events where the sign of the IMF $B_z$ component changed in a 10 min window, centered on the time of the neutral sheet crossing (from 5 min before the crossing to 5 min after).

Figure 4a shows how eliminating events during times of IMF $B_z$ sign changes affects the correlation and penetration efficiency as a function of lag time. Applying this criterion emphasizes the peak seen at around 4 h,

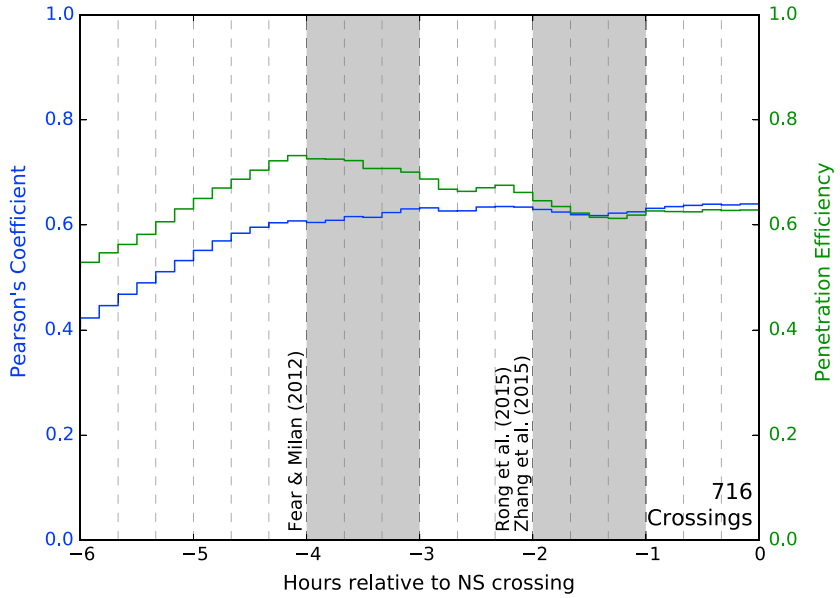


**Figure 5.** As in Figure 3, except that all of the criteria defined by *Cao et al.* [2014] have been applied.

but both peaks are still prominent. However, it generally has the effect of decreasing the penetration efficiency and correlation at shorter lag times (less than 4 h before the neutral sheet crossing), at which time both then follow a similar trace to that observed in the unfiltered data. The peaks in this plot occur at the same lag time as in the unfiltered data and have approximately the same value.

### 5.2. Solar Wind Pressure Pulse

In order to exclude disturbances due to sudden changes in solar wind pressure, *Cao et al.* [2014] also applied two solar wind pressure conditions based on absolute and relative changes in the pressure. Any crossing where there was a change in the solar wind pressure that was greater than 2 nPa or 50% within 5 min on either side of the crossing was excluded. Figure 4 shows how eliminating events which coincided with relative or absolute changes in the solar wind dynamical pressure of 2 nPa (Figure 4b1) or 50% (Figure 4b2) affects the lags. The peaks in each plot occur at the same lag time as in the unfiltered data and have approximately the same value. The rest of the traces follow a similar trend to that observed in the unfiltered data but at slightly lower values.

### 5.3. Fast Flows in the Magnetotail

The final condition applied by *Cao et al.* [2014] was the exclusion of neutral sheet crossings for which there was a simultaneous observation of a fast flow, exceeding 100 km $s^{-1}$, at the time of a neutral sheet crossing. Such a fast flow indicates the presence of a bursty bulk flow (BBF) which is associated with a dipolarization front [*Runov et al.*, 2009] and hence is likely to be associated with a variation in the magnetic field due to the reconfiguration of the magnetosphere and is therefore not in a steady state. In this instance the criterion was applied instantaneously (i.e., not within a 10 min window centered on the neutral sheet crossings).

Figure 4c shows the correlation and penetration over all lag times when fast flows in the magnetotail are not present. Applying this criterion has acted to increase the correlation at all lag times apart from close to the peak in Figure 3 at approximately 3 h 30 min, where it has remained the same. The peak in correlation occurs at 1 h 10 min with a value of 0.71 and the peak in penetration efficiency occurs at 3 h with a value of 0.72 although both traces now exhibit a very broad single peak. BBFs produce strong variations in the local magnetic field and so eliminating them reduces the scatter in the data, shown by the traces of penetration efficiency and correlation coefficient matching more closely than in the unfiltered data in Figure 3. In consistency with the analysis performed by *Cao et al.* [2014], each of the criteria was combined as shown in Figure 5. It can be seen, during periods of a quiet magnetotail, that the correlation is elevated for approximately 4 h before a neutral sheet crossing when the trace starts steadily decreasing; the penetration efficiency of the IMF into the magnetotail peaks at around 4 h before a neutral sheet crossing then decreases at around the same rate as the correlation coefficient.

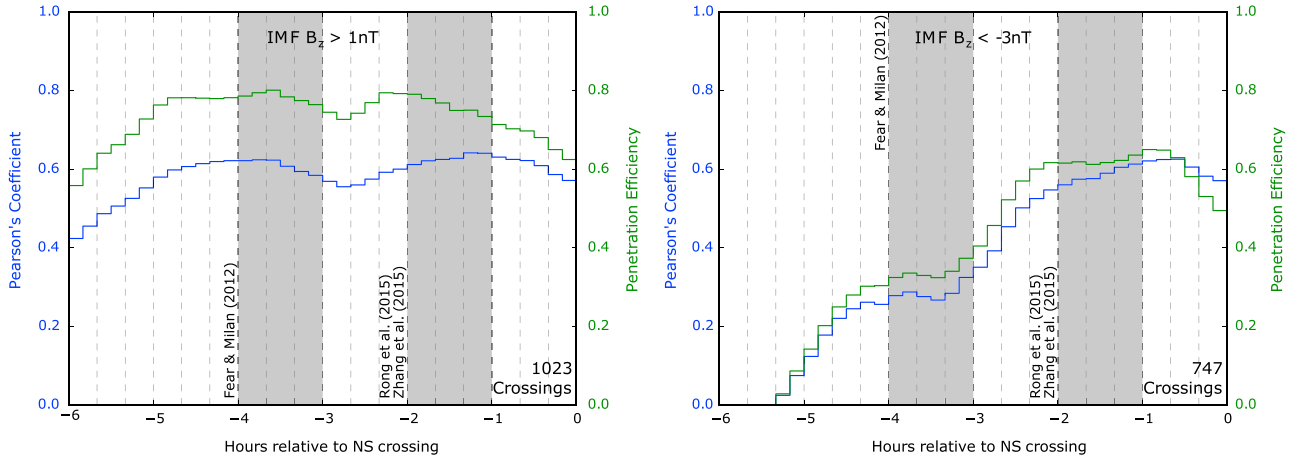


**Figure 6.** As in Figure 3, except with an IMF $B_z$ criterion applied. (left) The time series for events where IMF $B_z$ was "generally northward." A generally northward neutral sheet crossing was defined to be when 60% of the IMF $B_z$ data had been greater than 1 nT for 2 h leading up to the crossing. (right) The time series for events which occurred when the IMF was "generally southward." Similarly, a generally southward neutral sheet crossing was defined to be that when 60% of the IMF $B_z$ data had been less than −3 nT for 2 h leading up to the crossing. The correlation and penetration are elevated for a much longer time when IMF is northward compared to when IMF is negative.

## 6. Solar Wind Dependence

One would naturally expect the sign of the IMF $B_z$ component to exert an influence on the timescales associated with magnetospheric convection, and hence the distribution in Figure 3. *Cao et al.* [2014] sought to account for this factor by excluding neutral sheet crossings within 5 min of a sign change of the IMF $B_z$ component. We propose, however, that the time series of correlation and penetration efficiency should be more closely controlled by the sign of the IMF $B_z$ component rather than the presence or absence of sign changes. In order to filter separately periods of northward and southward IMF, we defined each neutral sheet crossing as occurring during a period of "generally northward" or "generally southward" IMF. Generally northward was defined to occur when more than 60% of the 1 min IMF $B_z$ data over 2 h leading up to the neutral sheet crossing was greater than 1nT, or less than −3 nT for generally southward IMF. (For clarity, we expect reconnection to take place under northward IMF conditions when the magnitude of IMF $B_y$ component dominates the IMF $B_z$ component [*Freeman et al.*, 1993].) The asymmetry in the criteria provides the best balance between being as strict as possible about which events were included without removing so many as to lose statistical validity. Figure 6 shows that periods of generally negative IMF $B_z$ give a relatively prompt response of approximately 1 h, compared to the time series plot for positive IMF $B_z$ where the correlation and penetration efficiency are both elevated for over 4 h before the neutral sheet crossing. It can also be seen in Figure 6 that the correlation coefficient matches the penetration efficiency much more closely than in Figure 3; we propose that this is due to the criteria eliminating sources of scatter.

As part of the hypothesis that the lag time would depend on dayside reconnection rate, the other factor which has to be taken into account is the solar wind velocity, as reflected by empirical expressions for the dayside reconnection rate [*Newell et al.*, 2007; *Milan et al.*, 2012; *Borovsky*, 2013]. If the solar wind is fast, then there will be a high arrival rate of IMF field lines at the magnetopause and therefore for a given reconnection efficiency, more field lines will have the opportunity to undergo reconnection; this in turn drives magnetospheric convection more rapidly than the opposite situation of slow solar wind conditions. Where the solar wind is slow, the IMF field lines are arriving at a slower rate and so dayside reconnection rate decreases, also decreasing the amount of driving in the magnetosphere. We therefore expect a more prompt response for fast solar wind speeds due to the increased driving of magnetospheric convection and a slower timescale for slower solar wind speeds. We test this hypothesis by defining crossings as being associated with periods of "generally slow" or "generally fast" solar wind speeds if more than 60% of the 1 min averaged solar wind velocity measurements from the 2 h leading up to the neutral sheet crossing were less than 400 km s$^{-1}$ or greater than 440 km s$^{-1}$, respectively. Again, boundaries are chosen so as not to eliminate too many neutral sheet crossings so that the statistical significance of the analysis remains high.

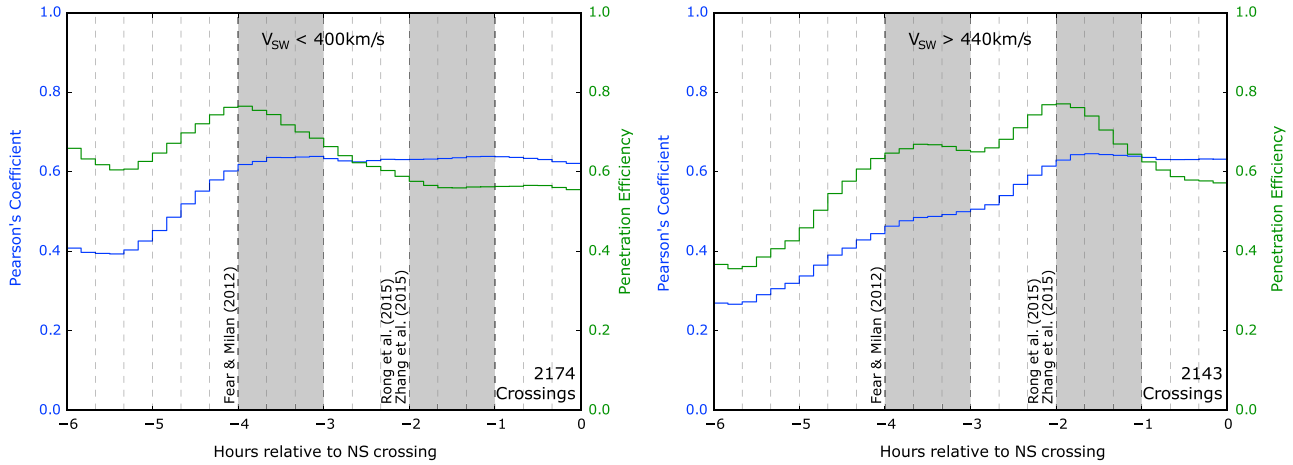


**Figure 7.** As in Figure 3, except with a solar wind velocity criteria applied. (left) The time series for events where the solar wind was "generally fast" (a minimum of 60% of the data over 2 h leading up to the neutral sheet crossing had to be >440 km $s^{-1}$) and (right) the time series for events when the solar wind was "generally slow" (a minimum of 60% of the data over 2 h leading up to the neutral sheet crossing had to be <400 km $s^{-1}$). The correlation and penetration are elevated for a much longer time when the solar wind is generally slow compared to when it is generally fast, when a much more prompt response is observed.

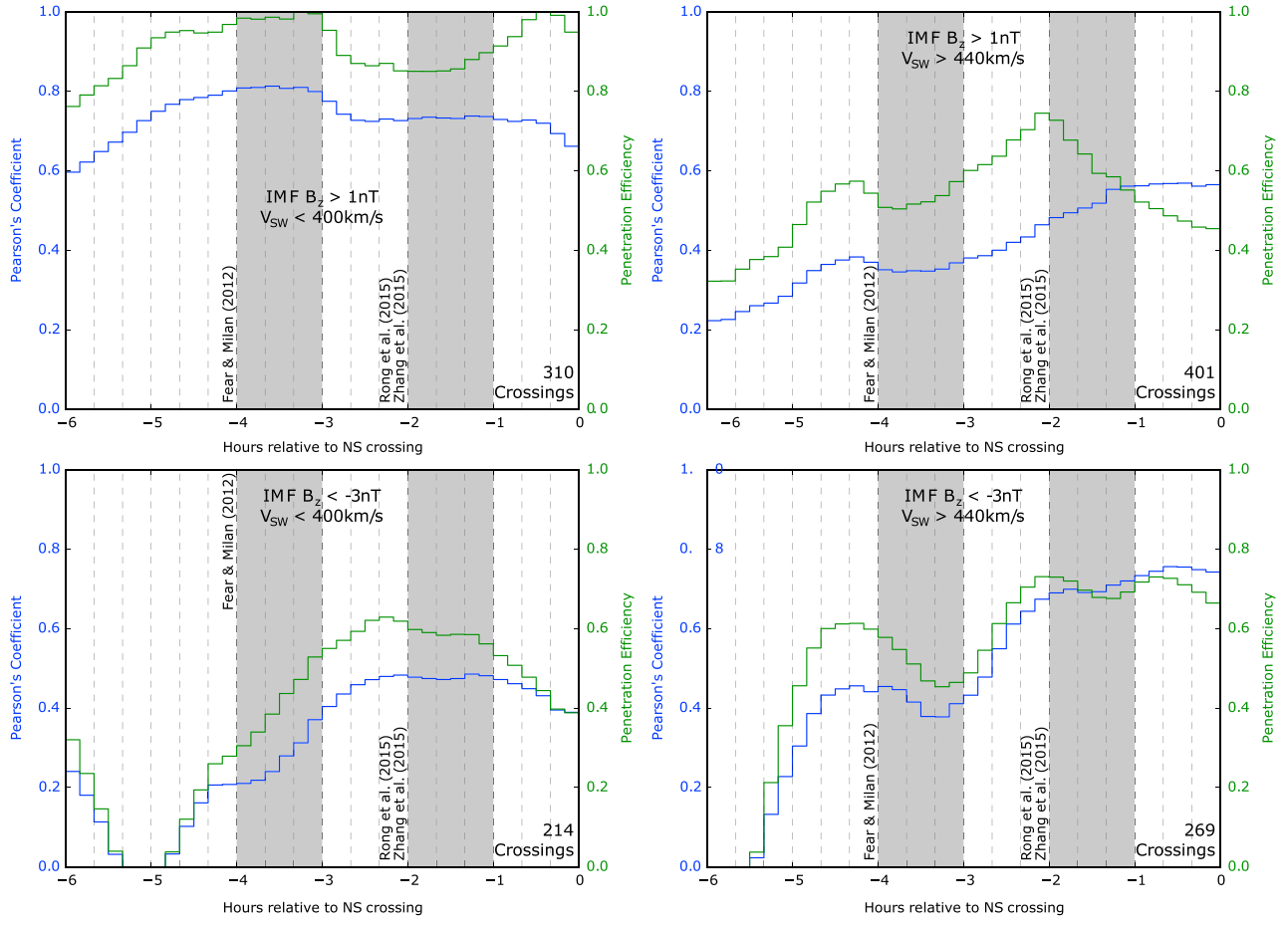


**Figure 8.** As in Figure 3, except that the criteria in the previous two figures have been combined. (top left) The correlation when dayside reconnection is unfavorable; a very long period of elevated correlation is observed. (bottom right) the correlation and penetration efficiency for events where dayside reconnection was highly favorable; a much more prompt correlation can be seen that decays quickly. (top right and bottom left) Events which satisfy the remaining combinations of each criteria; these show that the peaks in correlation lie between those found for events during times of favorable/unfavorable conditions for dayside reconnection to take place.

The results in Figure 7 show that for crossings associated with generally fast solar wind speeds, the correlation was elevated for 2 h immediately before the neutral sheet crossing whereas the correlation was elevated for approximately 4 h immediately before the crossings associated with slow solar wind speeds. The differences are starker in the behavior of the penetration efficiency, which peaks at about 2 h before the crossings for the fast solar wind speed events, and about 4 h before for the slow solar wind events. The plot for generally fast solar wind events shows a secondary peak at around 4 h which is only present in the penetration efficiency but coincides with a plateau in the correlation coefficient which is otherwise gradually decreasing. We conclude that this secondary feature is due to the threshold for "generally fast" solar wind not being set high enough; however, setting this value any higher rapidly decreases the statistical validity of the result.

In order to investigate if the peak in lag time depends on dayside reconnection rate, as predicted by empirical expressions, every combination of the IMF $B_z$ and solar wind speed criteria was applied to the data set of neutral sheet crossings, which is shown in Figure 8. We would expect the reconnection rate to be highest and hence the convection timescale fastest if IMF $B_z$ is negative and the solar wind is fast. If the IMF $B_z$ is positive and the solar wind speed is slow, we expect the reconnection rate to be slow and therefore the response time of the magnetotail also to be slow. The other combinations are expected to lie somewhere in between these two extreme conditions. Figure 8 (bottom right) shows that this is the case, with conditions most favorable for reconnection giving a response time of less than an hour, which then drops away after 2 h. Where reconnection is least favorable, shown in Figure 8 (top left), there is a peak in the correlation and penetration between 3 and 5 h. The other two panels in this Figure show traces of penetration efficiency and correlation that peak in between these two extremes as predicted. By applying the solar wind speed and IMF $B_z$ criteria we observe a much closer agreement between the traces of penetration efficiency and correlation coefficient which, as described earlier, indicates that scatter in the data has been reduced. These observations in Figure 8 fit well with the suggested mechanism that dayside reconnection rate drives magnetospheric convection and therefore influences how long it takes for the IMF to penetrate into closed field lines in the magnetotail.

## 7. Discussion

By taking magnetotail $B_Y$ data from all neutral sheet crossings that occurred during the observing region defined by *Cao et al.* [2014] and correlating these measurements with IMF $B_y$ data at increasing lag times, peaks in the correlation and penetration efficiency are observed, as seen in Figure 3. The locations at which previous studies have observed lag times coincide with peaks in the penetration efficiency and similar features in the correlation coefficient series.

To investigate what could be causing multiple timescales, we applied the criteria defined in *Cao et al.* [2014] to select neutral sheet crossing events that occurred during times of a quiet magnetosphere. Applying the same range of lag times to the solar wind data as was used for unfiltered events, a greater penetration of the IMF $B_y$ component into the $B_y$ component of the magnetotail is observed when a lag of approximately 4 h is applied (Figure 5). The correlation coefficient is elevated for 4 h before a neutral sheet crossing before decreasing, in agreement with the timescales observed in the penetration efficiency.

One of the criteria defined in *Cao et al.* [2014] was for no sign changes in IMF $B_z$. *Cao et al.* [2014] proposed this as *Keika et al.* [2008] and *Li et al.* [2011] have reported that initiating or halting dayside reconnection can introduce a perturbation in the magnetosphere which could affect the $B_y$ component measured in the magnetotail. We propose, however, that the sign of the IMF $B_z$ component has a greater effect on timescales than the presence of sign changes, because the sign of IMF $B_z$ largely controls the presence or absence of dayside reconnection, and hence the driving of the magnetosphere. We hypothesize that when magnetospheric convection is being driven, a more prompt timescale should be observed than when magnetospheric convection is stalled.

By taking northward IMF conditions to be when dayside reconnection is less favorable, it can be seen in Figure 6 (left) that the observations provide evidence for the hypothesis that a quiet magnetotail requires a longer time for the IMF to penetrate and then be removed from the magnetotail. The observed 4 h lag time is consistent with the value found by *Fear and Milan* [2012a] (3–4 h) when looking at the formation of transpolar arcs, which require northward IMF conditions. By taking events that occurred after a 2 h period of generally southward IMF conditions, a much more prompt peak is observed in both the correlation coefficient and penetration efficiency at approximately 40–60 min (Figure 6, right) which is consistent with the values found

by *Rong et al.* [2015] and *Zhang et al.* [2015] who were looking at events during periods of southward IMF conditions. The observed time lag during periods of southward IMF conditions is also consistent with reported timescales, associated with substorms such as the previous superposed epoch analysis by *Milan et al.* [2010], who showed that for 2000 substorms the time lag between there being a southward turning of the IMF relative to substorm onset was up to 2 h; also, observations by *Østgaard et al.* [2005] found that magnetotail twisting started to be influenced only 10 min after the arrival of IMF $B_y$. This window of 10 min to 2 h from *Østgaard et al.* [2005] and *Milan et al.* [2010], respectively, is consistent with an elevated correlation and penetration efficiency in Figure 6 (right) and also the hypothesis that during periods of high magnetospheric driving caused by a high dayside reconnection rate, the timescale for magnetospheric convection, and therefore timescales for the penetration of the IMF $B_y$ component into the magnetosphere, is low. The difference in timescales between southward and northward IMF conditions (shown in Figure 6) allows us to draw a synthesis between the two phenomena of substorms [*Milan et al.*, 2010] and transpolar arcs [*Fear and Milan*, 2012a], both of which are caused by magnetotail reconnection but under IMF conditions that are preferential for high and low magnetospheric driving, respectively, and have exhibited timescales consistent with those found in this study for their required IMF conditions.

The hypothesis was further tested by examining how timescales depend on the solar wind speed. An effect might be expected, as the dayside reconnection rate is partly controlled by the solar wind speed [*Newell et al.*, 2007; *Milan et al.*, 2012; *Borovsky*, 2013]. As described in the previous section, we expect slow solar wind to indicate times of a low dayside reconnection rate and therefore a quiet magnetosphere, requiring longer timescales for IMF penetration. Oppositely, during times of fast solar wind speed, the dayside reconnection rate will be higher, and therefore, magnetospheric convection will be more active giving a more prompt response time of the magnetosphere to the IMF. In a similar way to our approach of examining periods of "generally southward" and "generally northward" IMF $B_z$ conditions, the solar wind was filtered to find times of "generally fast" or "generally slow" solar wind over 2 h leading up to the neutral sheet crossing. Figure 7 shows that for slow solar wind, a long timescale is observed of approximately 4 h where the correlation coefficient is elevated, and the penetration efficiency peaks at that time. This timescale is similar to that observed for northward IMF conditions, when dayside reconnection is also less favorable. As expected, fast solar wind conditions exhibit a much more prompt response time of approximately 2 h, where the penetration efficiency peaks and the correlation coefficient is elevated up to this lag time.

The plots from Figure 8 show that by selecting neutral sheet crossings that occurred under certain solar wind conditions related to the dayside reconnection rate, a change in the response time of the neutral sheet is observed. When the expected dayside reconnection rate is low (Figure 8, top left), a long lag time is again observed which is consistent with the previous result in this study and the result found by *Fear and Milan* [2012a]. When the dayside reconnection rate is high, however (Figure 8, bottom right), a much more prompt response is found where the penetration efficiency exhibits a broad peak at approximately 40 min to 2 h before sharply decreasing; the correlation coefficient indicates that there is the least amount of scatter on the data at approximately 40 min and remains elevated for up to 2 h, which is more consistent with values found by *Rong et al.* [2015] and *Zhang et al.* [2015].

*Tenfjord et al.* [2015] suggest that when dayside reconnection occurs during conditions of IMF $B_y \neq 0$, there are asymmetries between the density of field lines in the dusk/dawn sectors of the northern and southern hemispheres. This asymmetric addition of flux imparts a pressure upon the magnetotail which causes it to reconfigure to a state which is consistent with the IMF including its $B_y$ component. Simulations run by *Tenfjord et al.* [2015] have estimated that this reconfiguration will begin after approximately 25 mins and, if significant, should also correspond to the lag time which gives rise to peaks in the penetration efficiency and correlation coefficient; however, our results are not consistent with this scenario. While there may be an MHD pressure wave that causes the magnetotail to reconfigure to IMF conditions more rapidly than by the convection of field lines, its significance (compared to a $B_y$ component induced from field line convection) is low and cannot be seen above the background correlation which we propose is due to the finite timescales by which the solar wind varies. Oppositely, observations have been reported that the IMF $B_y$ component has to have either positive or negative values for up to a day to fully have an effect on the onset MLT location of substorms [*Milan et al.*, 2010]; similarly, *Grocott and Milan* [2014] have reported that the shape of the ionospheric convection patterns are still being altered after 10 h when there has been a persistent IMF $B_y$ component. The mechanism behind these longer timescales is unknown.

**Table 1.** Estimates for the Field Line Convection Time Over the Polar Cap

| | Field Line Convection Speed | | |
|---|---|---|---|
| | 240 m/s | 330 m/s | 440 m/s |
| $Area_{pc}$ | | | |
| $9.4 \times 10^{12}$ m$^2$ | 4 h | 2 h 50 min | 2 h 10 min |
| $1.1 \times 10^{13}$ m$^2$ | 4 h 20 min | 3 h 10 min | 2 h 20 min |
| $1.4 \times 10^{13}$ m$^2$ | 5 h | 3 h 30 min | 2 h 40 min |

It has been estimated that the timescale for the penetration of the IMF into the magnetotail should take of the order of hours [*Dungey*, 1965; *Cowley*, 1981b; *Fear and Milan*, 2012a], based on the time taken for the ionospheric end of an open field line to cross the polar cap. In Table 1, we develop this idea further by using the distribution of polar cap areas reported by *Milan et al.* [2007] and a distribution of polar cap convection speed vectors observed near the pole in the midnight sector [*Grocott et al.*, 2009] by SuperDARN [*Greenwald et al.*, 1995; *Chisham et al.*, 2007]. The ionospheric convection speeds were calculated from the two-dimensional ionospheric velocity vectors which were derived using the map potential technique [*Ruohoniemi and Baker*, 1998] within an ~500 × 500 km box, centered at a latitude of ~83° at midnight MLT (magnetic local time). The precise location of the box is scaled to the zero potential boundary, and the precise size of the box scales accordingly. The reader is referred to *Grocott et al.* [2009] for a more detailed description of the statistical database used (the box in question is no. 33 from Figure 2 in their paper). The speeds used are averages of at least two measurements located within the box; one average speed value was calculated for each 2 min interval between 1999 and 2006 for which there were at least two points of ionospheric scatter in the box. Figure 9 (left) shows the occurrence of ionospheric convection speeds binned in 50 m s$^{-1}$ increments; in this figure, any flows where the corresponding vector has a sunward component have been removed. Figure 9 (right) shows occurrence of polar cap diameters binned in 500 km increments, converted from the areas reported in Figure 3 of *Milan et al.* [2007]. Using the mode field line convection speed of 330 m s$^{-1}$ and the mode polar cap area of $1.1 \times 10^{13}$ m$^2$ (Figure 9) [*Milan et al.*, 2003, 2007, 2009], giving a cross polar cap distance of approximately 3800 km, we estimate the time taken for a field line to be transported through the lobe to be approximately 3 h (Table 1, center cell). This estimate compares well with the *Cowley* [1981b] and *Fear and Milan* [2012a] estimates, based on similar calculations. By taking the lower and upper quartiles of convection speeds (240 m s$^{-1}$ and 440 m s$^{-1}$, respectively), and polar cap areas (9.4 and $14 \times 10^{12}$ km$^2$, respectively—Figure 9), Table 1 shows how the timescale for convection of field lines from the dayside magnetopause to the lobe-plasma sheet boundary might be expected to vary from ~2 to 5 h. As our observations are taken from the neutral sheet, we expect these calculations to be a slight underestimate; this is because

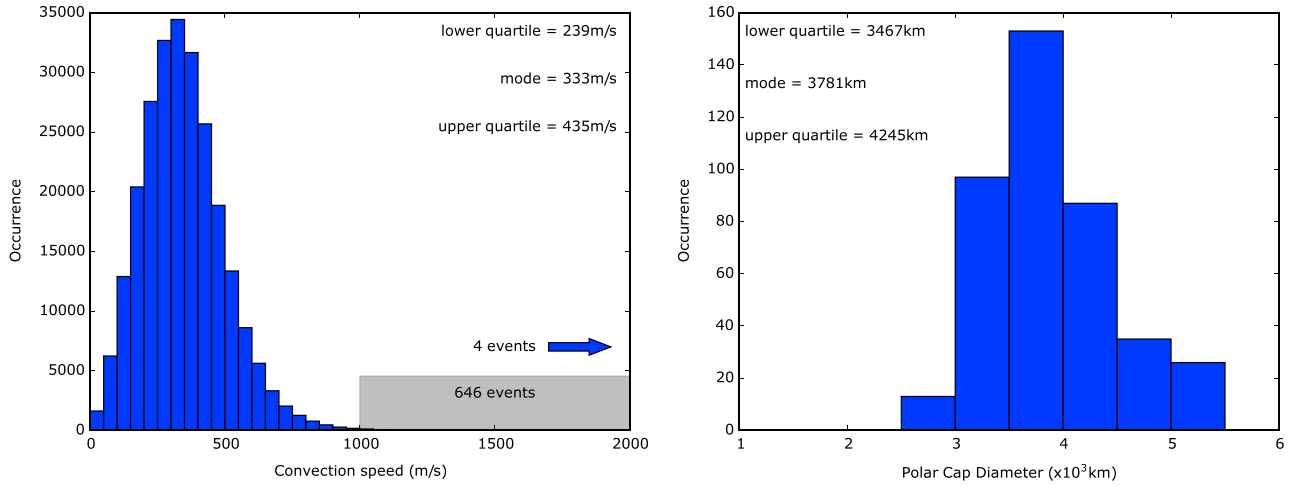


**Figure 9.** (left) Occurrences of ionospheric convection speeds in the midnight sector at approximately 85° of latitude, as measured by SuperDARN from 1999 to 2006. (right) The occurrences of the diameter of the polar cap over a total of 73 h of observations taken between 1998 and 2002 during a variety of geophysical conditions; these data are reproduced from Figure 3 of *Milan et al.* [2007], but the *x* axis values of magnetic flux content have been converted to polar cap diameter.

the spacecraft measures the neutral sheet earthward of the tail *x*!line, and so the field lines have convected further (and for longer) than we have accounted for in the calculation. It can be seen that the estimate for the upper limit of magnetospheric convection always contains the peak in correlation and penetration in all lag time figures (Figures 3–8).

## 8. Conclusion

In this study we have presented statistical evidence for the timescales associated with the penetration of the IMF into the neutral sheet. We find two distinct timescales close to 2 h and 4 h which are consistent with estimates for timescales found by previous studies for southward and northward IMF, respectively. Events were then filtered by whether the event occurred during "generally northward" or "generally southward" IMF conditions. When the IMF was generally southward the response time of the plasma sheet to the penetration of IMF $B_y$ was around 1–2 h; when the IMF was generally northward, the plasma sheet was correlated for up to 5 h. During generally fast solar wind conditions there was a response time of ~2 h for the IMF $B_y$ to enter the plasma sheet, and under generally slow solar wind conditions the plasma sheet was observed to correlate with the IMF for up to 4 h beforehand, with a peak in the penetration efficiency at ~4 h.

By applying criteria to the sign on the IMF $B_z$ component and the solar wind speed, we found that the relative heights of the peaks in correlation and penetration efficiency changed based on the strength of the magnetospheric driving. By combining the IMF $B_z$ and solar wind speed criteria, we expect the penetration timescale to vary if penetration is controlled by dayside reconnection rate, as dayside reconnection is the primary mechanism behind magnetospheric driving. We found that when the dayside reconnection rate is high (therefore, magnetospheric driving is high), there is a much more rapid response of the neutral sheet to changes in the IMF conditions of the order of 1–2 h; conversely, when the dayside reconnection rate is low (low magnetospheric driving) there was a much longer timescale associated with IMF penetration of the order of 3–5 h. Our observed timescales are consistent with the range expected from calculations based on arguments by *Dungey* [1965] (see our Table 1).

**Acknowledgments**
Cluster data were obtained from the Cluster Active Archive (http://caa.estec.esa.int/caa/). The OMNI data were obtained from the SPDF OMNIWeb interface at http://omniweb.gsfc.nasa.gov. S.D.B. was supported by Science and Technology Facilities Council (STFC) studentship ST/M503794/1 R.C.F. was supported by STFC Ernest Rutherford Fellowship ST/K004298/2. A.G. was supported by STFC grant ST/M001059/1. S.E.M. was supported by STFC grant ST/N000749/1. The work at the Birkeland Centre for Space Centre, University of Bergen, Norway, was supported by the Research Council of Norway/CoE under contract 223252/F50. R.C.F. would like to thank Oscar Miles and Natasha Dell for their preliminary work on this project. S.D.B. would also like to thank Paul Tenfjord from the University of Bergen for providing feedback and his insight.

## References

Balogh, A., et al. (2001), The Cluster magnetic field investigation: Overview of in-flight performance and initial results, *Ann. Geophys.*, *19*, 1207–1217, doi:10.5194/angeo-19-1207-2001.

Borovsky, J. E. (2013), Physical improvements to the solar wind reconnection control function for the Earth's magnetosphere, *J. Geophys. Res. Space Physics*, *118*, 2113–2121, doi:10.1002/jgra.50110.

Cao, J., A. Duan, H. Reme, and I. Dandouras (2013), Relations of the energetic proton fluxes in the central plasma sheet with solar wind and geomagnetic activities, *J. Geophys. Res. Space Physics*, *118*, 7226–7236, doi:10.1002/2013JA019289.

Cao, J., A. Duan, M. Dunlop, X. Wei, and C. Cai (2014), Dependence of IMF $B_y$ penetration into the neutral sheet on IMF $B_z$ and geomagnetic activity, *J. Geophys. Res. Space Physics*, *119*, 5279–5285, doi:10.1002/2014JA019827.

Chisham, G., et al. (2007), A decade of the Super Dual Auroral Radar Network (SuperDARN): Scientific achievements, new techniques and future directions, *Surv. Geophys.*, *28*, 33–109, doi:10.1007/s10712-007-9017-8.

Cowley, S. W. H. (1981a), Magnetospheric asymmetries associated with the *y*-component of the IMF, *Planet. Space Sci.*, *29*, 79–96, doi:10.1016/0032-0633(81)90141-0.

Cowley, S. W. H. (1981b), Magnetospheric and ionospheric flow and the interplanetary magnetic field, in *Physical basis of the Ionosphere in the Solar-Terrestrial System*, AGARD CP-295, pp. 4.1–4.14, Advisory Group for Aerospace Res. and Dev., NATO, Neuilly sur Seine, France.

Dandouras, I., A. Barthe, E. Penou, S. Brunato, H. Rème, L. M. Kistler, M. B. Bavassano-Cattaneo, and A. Blagau (2010), Cluster Ion Spectrometry (CIS) Data in the Cluster Active Archive (CAA), *Astrophys. Space Sci. Proc.*, *11*, 51–72, doi:10.1007/978-90-481-3499-13.

Dungey, J. W. (1961), Interplanetary magnetic field and the auroral zones, *Phys. Rev. Lett.*, *6*, 47–48, doi:10.1103/PhysRevLett.6.47.

Dungey, J. W. (1965), The length of the magnetospheric tail, *J. Geophys. Res.*, *70*, 1753–1753, doi:10.1029/JZ070i007p01753.

Fairfield, D. H. (1979), On the average configuration of the geomagnetic tail, *J. Geophys. Res.*, *84*, 1950–1958, doi:10.1029/JA084iA05p01950.

Fear, R. C., and S. E. Milan (2012a), The IMF dependence of the local time of transpolar arcs: Implications for formation mechanism, *J. Geophys. Res.*, *117*, A03213, doi:10.1029/2011JA017209.

Fear, R. C., and S. E. Milan (2012b), Ionospheric flows relating to transpolar arc formation, *J. Geophys. Res.*, *117*, A09230, doi:10.1029/2012JA017830.

Frank, L. A., J. D. Craven, J. L. Burch, and J. D. Winningham (1982), Polar views of the Earth's aurora with dynamics explorer, *Geophys. Res. Lett.*, *9*(9), 1001–1004, doi:10.1029/GL009i009p01001.

Freeman, M. P., C. J. Farrugia, L. F. Burlaga, M. R. Hairston, M. E. Greenspan, J. M. Ruohoniemi, and R. P. Lepping (1993), The interaction of a magnetic cloud with the Earth—Ionospheric convection in the Northern and Southern Hemispheres for a wide range of quasi-steady interplanetary magnetic field conditions, *J. Geophys. Res.*, *98*, 7633–7655, doi:10.1029/92JA02350.

Gloag, J. M., E. A. Lucek, L.-N. Alconcel, A. Balogh, P. Brown, C. M. Carr, C. N. Dunford, T. Oddy, and J. Soucek (2010), FGM data products in the CAA, in *The Cluster Active Archive—Studying the Earth's Space Plasma Environment*, edited by H. Laakso, M. Taylor, and P. Escoubet, pp. 109–128, Springer, Dordrecht, Netherlands, doi:10.1007/978-90-481-3499-1/7.

Greenwald, R. A., et al. (1995), DARN/SuperDARN: A global view of the dynamics of high-lattitude convection, *Space Sci. Rev.*, *71*, 761–796, doi:10.1007/BF00751350.

Grocott, A., and S. E. Milan (2014), The influence of IMF clock angle timescales on the morphology of ionospheric convection, *J. Geophys. Res. Space Physics*, *119*, 5861–5876, doi:10.1002/2014JA020136.

Grocott, A., J. A. Wild, S. E. Milan, and T. K. Yeoman (2009), Superposed epoch analysis of the ionospheric convection evolution during substorms: Onset latitude dependence, *Ann. Geophys.*, *27*, 591–600, doi:10.5194/angeo-27-591-2009.

Hau, L.-N., and G. M. Erickson (1995), Penetration of the interplanetary magnetic field $B_y$ into Earth's plasma sheet, *J. Geophys. Res.*, *100*, 21,745–21,752, doi:10.1029/95JA01935.

Hilmer, R. V., and G.-H. Voigt (1987), The effects of magnetic $B_y$ component on geomagnetic tail equilibria, *J. Geophys. Res.*, *92*, 8660–8672, doi:10.1029/JA092iA08p08660.

Kaymaz, Z., G. L. Siscoe, J. G. Luhmann, R. P. Lepping, and C. T. Russell (1994), Interplanetary magnetic field control of magnetotail magnetic field geometry: IMP 8 observations, *J. Geophys. Res.*, *99*, 11,113–11,126, doi:10.1029/94JA00300.

Keika, K., et al. (2008), Response of the inner magnetosphere and the plasma sheet to a sudden impulse, *J. Geophys. Res.*, *113*, A07S35, doi:10.1029/2007JA012763.

King, J. H., and N. E. Papitashvili (2005), Solar wind spatial scales in and comparisons of hourly Wind and ACE plasma and magnetic field data, *J. Geophys. Res.*, *110*, A02104, doi:10.1029/2004JA010649.

Li, L. Y., et al. (2011), Multiple responses of magnetotail to the enhancement and fluctuation of solar wind dynamic pressure and the southward turning of interplanetary magnetic field, *J. Geophys. Res.*, *116*, A12223, doi:10.1029/2011JA016816.

Milan, S. E., M. Lester, S. W. H. Cowley, K. Oksavik, M. Brittnacher, R. A. Greenwald, G. Sofko, and J.-P. Villain (2003), Variations in the polar cap area during two substorm cycles, *Ann. Geophys.*, *21*, 1121–1140, doi:10.5194/angeo-21-1121-2003.

Milan, S. E., B. Hubert, and A. Grocott (2005), Formation and motion of a transpolar arc in response to dayside and nightside reconnection, *J. Geophys. Res.*, *110*, A01212, doi:10.1029/2004JA010835.

Milan, S. E., G. Provan, and B. Hubert (2007), Magnetic flux transport in the Dungey cycle: A survey of dayside and nightside reconnection rates, *J. Geophys. Res.*, *112*, A01209, doi:10.1029/2006JA011642.

Milan, S. E., J. Hutchinson, P. D. Boakes, and B. Hubert (2009), Influences on the radius of the auroral oval, *Ann. Geophys.*, *27*, 2913–2924, doi:10.5194/angeo-27-2913-2009.

Milan, S. E., A. Grocott, and B. Hubert (2010), A superposed epoch analysis of auroral evolution during substorms: Local time of onset region, *J. Geophys. Res.*, *115*, A00I04, doi:10.1029/2010JA015663.

Milan, S. E., J. S. Gosling, and B. Hubert (2012), Relationship between interplanetary parameters and the magnetopause reconnection rate quantified from observations of the expanding polar cap, *J. Geophys. Res.*, *117*, A03226, doi:10.1029/2011JA017082.

Moses, J. J., N. U. Crooker, D. J. Gorney, and G. L. Siscoe (1985), High-latitude convection on open and closed field lines for large IMF $B_y$, *J. Geophys. Res.*, *90*, 11,078–11,082, doi:10.1029/JA090iA11p11078.

Nagai, T. (1987), Interplanetary magnetic field $B_y$ effects on the magnetic field at synchronous orbit, *J. Geophys. Res.*, *92*, 11,215–11,220, doi:10.1029/JA092iA10p11215.

Newell, P. T., D. G. Sibeck, and C.-I. Meng (1995), Penetration of the interplanetary magnetic field $B_y$ magnetosheath plasma into the magnetosphere: Implications for the predominant magnetopause merging site, *J. Geophys. Res.*, *100*, 235–243, doi:10.1029/94JA02632.

Newell, P. T., T. Sotirelis, K. Liou, C.-I. Meng, and F. J. Rich (2007), A nearly universal solar wind-magnetosphere coupling function inferred from 10 magnetospheric state variables, *J. Geophys. Res.*, *112*, A01206, doi:10.1029/2006JA012015.

Nishida, A., and T. Ogino (1998), Convection and reconnection in the Earth's magnetotail, in *New Perspectives on the Earth'S Magnetotail, Geophys. Monogr. Ser.*, vol. 105, pp. 61–76, AGU, Washington, D. C.

Nishida, A., T. Mukai, T. Yamamoto, Y. Saito, S. Kokubun, and K. Maezawa (1995), GEOTAIL observation of magnetospheric convection in the distant tail at 200 $R_E$ in quiet times, *J. Geophys. Res.*, *100*, 23,663–23,676, doi:10.1029/95JA02519.

Nishida, A., T. Mukai, T. Yamamoto, S. Kokubun, and K. Maezawa (1998), A unified model of the magnetotail convection in geomagnetically quiet and active times,*J. Geophys. Res.*, *103*, 4409–4418, doi:10.1029/97JA01617.

Østgaard, N., N. A. Tsyganenko, S. B. Mende, H. U. Frey, T. J. Immel, M. Fillingim, L. A. Frank, and J. B. Sigwarth (2005), Observations and model predictions of substorm auroral asymmetries in the conjugate hemispheres,*Geophys. Res. Lett.*, *32*, L05111, doi:10.1029/2004GL022166.

Petrukovich, A. A. (2009), Dipole tilt effects in plasma sheet $B_y$: Statistical model and extreme values, *Ann. Geophys.*, *27*, 1343–1352, doi:10.5194/angeo-27-1343-2009.

Petrukovich, A. A. (2011), Origins of plasma sheet $B_y$, *J. Geophys. Res.*, *116*, A07217, doi:10.1029/2010JA016386.

Rème, H., et al. (2001), First multispacecraft ion measurements in and near the Earth's magnetosphere with the identical Cluster ion spectrometry (CIS) experiment, *Ann. Geophys.*, *19*, 1303–1354, doi:10.5194/angeo-19-1303-2001.

Rong, Z. J., A. T. Y. Lui, W. X. Wan, Y. Y. Yang, C. Shen, A. A. Petrukovich, Y. C. Zhang, T. L. Zhang, and Y. Wei (2015), Time delay of interplanetary magnetic field penetration into Earth's magnetotail, *J. Geophys. Res. Space Physics*, *120*, 3406–3414, doi:10.1002/2014JA020452.

Runov, A., V. Angelopoulos, M. I. Sitnov, V. A. Sergeev, J. Bonnell, J. P. McFadden, D. Larson, K.-H. Glassmeier, and U. Auster (2009), THEMIS observations of an earthward-propagating dipolarization front, *Geophys. Res. Lett.*, *36*, L14106, doi:10.1029/2009GL038980.

Ruohoniemi, J. M., and K. B. Baker (1998), Large-scale imaging of high-latitude convection with Super Dual Auroral Radar Network HF radar observations, *J. Geophys. Res.*, *103*, 20,797–20,811, doi:10.1029/98JA01288.

Sergeev, V. A. (1987), Penetration of the $B_y$ component of the IMF into the magnetotail, *Geomagn. Aeron.*, *27*, 612–615.

Tenfjord, P., N. Østgaard, K. Snekvik, K. M. Laundal, J. P. Reistad, S. Haaland, and S. E. Milan (2015), How the IMF $B_y$ induces a $B_y$ component in the closed magnetosphere and how it leads to asymmetric currents and convection patterns in the two hemispheres, *J. Geophys. Res. Space Physics*, *120*, 9368–9384, doi:10.1002/2015JA021579.

Tsurutani, B. T., E. J. Smith, D. E. Jones, R. P. Lepping, and D. G. Sibeck (1984), The relationship between the IMF $B_y$ and the distant tail (150–238 $R_e$) lobe and plasmasheet $B_y$ fields, *Geophys. Res. Lett.*, *11*, 1082–1085, doi:10.1029/GL011i010p01082.

Voigt, G.-H., and R. V. Hilmer (1987), The influence of the IMF $B_y$ component on the Earth's magneto-hydrostatic magnetotail, in *Magnetotail Physics*, edited by A. T. Y. Lui and S.-I. Akasofu, pp. 91–97, Johns Hopkins Univ. Press, Baltimore, Md.

Wing, S., P. T. Newell, D. G. Sibeck, and K. B. Baker (1995), A large statistical study of the entry of interplanetary magnetic field $Y$-component into the magnetosphere, *Geophys. Res. Lett.*, *22*, 2083–2086, doi:10.1029/95GL02261.

Zhang, Q.-H., M. Lockwood, J. C. Foster, S.-R. Zhang, B.-C. Zhang, I. W. McCrea, J. Moen, M. Lester, and J. M. Ruohoniemi (2015), Direct observations of the full Dungey convection cycle in the polar ionosphere for southward interplanetary magnetic field conditions, *J. Geophys. Res. Space Physics*, *120*, 4519–4530, doi:10.1002/2015JA021172.